

Reactions of Laser-Ablated La and Y Atoms with CO: Matrix Infrared Spectra and DFT Calculations of the $M(\text{CO})_x$ and MCO^+ ($M = \text{La}, \text{Y}; x = 1-4$) Molecules

Ling Jiang and Qiang Xu*

National Institute of Advanced Industrial Science and Technology (AIST), Ikeda, Osaka 563-8577, Japan, and Graduate School of Science and Technology, Kobe University, Nada Ku, Kobe, Hyogo 657-8501, Japan

Received: December 5, 2006; In Final Form: February 28, 2007

Reactions of laser-ablated lanthanum and yttrium atoms with carbon monoxide molecules in solid neon have been investigated using matrix-isolation infrared spectroscopy. The $M(\text{CO})_x$ and MCO^+ ($M = \text{La}, \text{Y}; x = 1-4$) molecules have been formed and identified on the basis of isotopic shifts, mixed isotopic splitting patterns, and CCl_4 -doping experiments. Density functional theory calculations have been performed on these lanthanum and yttrium carbonyls. The agreement between the experimental and calculated vibrational frequencies, relative absorption intensities, and isotopic shifts substantiates the identification of these carbonyls from the matrix infrared spectrum. The present study reveals that the C–O stretching vibrational frequencies of MCO^+ decrease from Sc to La, which indicates an increasing in metal d orbital \rightarrow CO π^* back-donation in this series.

Introduction

The interaction of metal atoms with small molecules (i.e., CO, O₂, CO₂, H₂, CH₄, etc.) is of considerable interest because of its importance in a great number of catalytic processes.¹ Among these small molecules, carbon monoxide is one of the most important in transition-metal chemistry from an academic or an industrial viewpoint.^{1,2} Reactions of various transition-metal and main-group metal atoms with carbon monoxide have been investigated and a series of metal carbonyl complexes have been experimentally characterized.^{3–5} Quantum chemical calculations have been performed to understand the electronic structures and bonding characteristics of metal carbonyls complexes.^{3,4,6,7}

Recent studies have shown that, with an aid of isotopic substitution technique, matrix isolation infrared spectroscopy combined with quantum chemical calculation is very powerful in investigating the spectrum, structure and bonding of novel species.^{3,4,8,9} Taking the group 3 metal carbonyls as an example, the $\text{Sc}(\text{CO})_x$ ($x = 1-4$), ScCO^+ , ScCO^- , $\text{Sc}_2[\eta^2(\mu_2\text{-C}, \text{O})]$, and $c\text{-Sc}_2(\mu\text{-C})(\mu\text{-O})$ molecules have been observed in the argon and neon matrices.^{10,11} Argon matrix investigations of the reaction of laser-ablated La atoms and CO molecules have characterized the neutral monocarbonyl LaCO and the $\text{La}_2[\eta^2(\mu_2\text{-C}, \text{O})]$ and $c\text{-La}_2(\mu\text{-C})(\mu\text{-O})$ molecules.¹² The analogous $c\text{-Y}_2(\mu\text{-C})(\mu\text{-O})$ molecule has been identified from isotopic shifts and splitting patterns in the argon matrix infrared spectra.¹³ Two sets of broad bands at 1874.1, 1869.0 and 1909.4, 1903.6, 1893.3 cm^{-1} have been assigned to the YCO and YCO^+ molecules in the previous argon matrix experiments, respectively.¹⁰ However, much less work has been done on higher lanthanum or yttrium carbonyls. Considering that solid neon may stabilize some species difficult to be observed in solid argon,^{3,4} we have performed the reactions of laser-ablated lanthanum and yttrium atoms with CO molecules in excess neon. IR spectroscopy coupled with theoretical calculations provides evidence for the formation of the $M(\text{CO})_x$ and MCO^+ ($M = \text{La}, \text{Y}; x = 1-4$) molecules.

Experimental and Theoretical Methods

The experiment for laser ablation and matrix isolation infrared spectroscopy is similar to those previously reported.^{14,15} In short, the Nd:YAG laser fundamental (1064 nm, 10 Hz repetition rate with 10 ns pulse width) was focused on the rotating La and Y targets. The laser-ablated La and Y atoms were co-deposited with CO in excess neon onto a CsI window cooled normally to 4 K by means of a closed-cycle helium refrigerator. Typically, 1–8 mJ/pulse laser power was used. CO (99.95%), ¹³C¹⁶O (99%, ¹⁸O < 1%), and ¹²C¹⁸O (99%) were used to prepare the CO/Ne mixtures. In general, matrix samples were deposited for 30–60 min with a typical rate of 2–4 mmol per hour. After sample deposition, IR spectra were recorded on a BIO-RAD FTS-6000e spectrometer at 0.5 cm^{-1} resolution using a liquid nitrogen cooled HgCdTe (MCT) detector for the spectral range of 5000–400 cm^{-1} . Samples were annealed at different temperatures and subjected to broad-band irradiation ($\lambda > 250$ nm) using a high-pressure mercury arc lamp (Ushio, 100 W).

Density functional theory (DFT) calculations were performed to predict the structures and vibrational frequencies of the observed reaction products using the Gaussian 03 program.¹⁶ Note that the BPW91 functional gives calculated $\nu_{\text{C-O}}$ frequencies for lanthanum and yttrium carbonyls much closer to the experimental values than the BP86 functional.^{12,13} Herein, most calculations employed the BPW91 density functional method but comparisons were done with the B3LYP density functional method as well.¹⁷ The 6-31+G(d) basis set was used for C and O atoms,¹⁸ and the Stevens/Basch/Krauss ECP split valance (CEP-31G) for La and Y atoms.¹⁹ Geometries were fully optimized and vibrational frequencies were calculated with analytical second derivatives. The previous investigations have shown that such computational methods can provide reliable information for metal carbonyls, such as infrared frequencies, relative absorption intensities, and isotopic shifts.^{3,4,11–13}

Results and Discussion

Experiments have been done with carbon monoxide concentrations ranging from 0.02% to 1.0% in excess neon. Typical

* Corresponding author. E-mail: q.xu@aist.go.jp.

TABLE 1: Infrared Absorptions (cm⁻¹) Observed from the Reactions of Laser-Ablated La Atoms with CO in Excess Neon at 4 K

¹² C ¹⁶ O	¹³ C ¹⁶ O	¹² C ¹⁸ O	¹² C ¹⁶ O + ¹³ C ¹⁶ O	¹² C ¹⁶ O + ¹² C ¹⁸ O	<i>R</i> (12/13)	<i>R</i> (16/18)	assignment
1983.3	1940.7	1934.9			1.0220	1.0250	(La(CO) ₆) site
1977.1	1934.1	1929.2			1.0222	1.0248	(La(CO) ₆)
1940.3	1897.4	1892.0			1.0226	1.0255	(La(CO) ₅)
1919.9	1879.0	1873.0			1.0218	1.0250	La(CO) ₃
1903.2	1862.0	1859.1	1903.2, 1862.0	1903.2, 1859.1	1.0221	1.0237	LaCO ⁺
1882.1	1841.5	1836.3	1882.1, 1869.1, 1858.0, 1849.9, 1841.6	1882.1, 1866.7, 1854.8, 1845.6, 1836.3	1.0220	1.0249	La(CO) ₄
1849.9	1808.9	1806.4	1849.8, 1833.3, 1822.7, 1809.3	1850.0, 1833.0, 1821.0, 1807.2	1.0227	1.0241	La(CO) ₃
1833.6	1794.5	1788.9	1833.3, 1794.8	1833.0, 1788.2	1.0218	1.0250	LaCO site
1814.0	1774.2	1770.6	1813.9, 1774.3	1814.0, 1771.9	1.0224	1.0245	LaCO
1788.2	1749.9	1744.5	1788.2, 1764.0, 1749.9	1788.2, 1760.6, 1744.6	1.0219	1.0251	La(CO) ₂ (linear)
1776.0	1737.6	1732.9	1774.3, 1754.8, 1737.9	1775.9, 1751.7, 1733.6	1.0221	1.0249	La(CO) ₂ (bent)
1745.6	1708.4	1702.6	1745.7, 1723.4, 1708.5	1744.6, 1720.0, 1703.0	1.0218	1.0253	La(CO) ₂ (bent)

TABLE 2: Infrared Absorptions (cm⁻¹) Observed from the Reactions of Laser-Ablated Y Atoms with CO in Excess Neon at 4 K

¹³ C ¹⁶ O	¹³ C ¹⁶ O	¹² C ¹⁸ O	¹² C ¹⁶ O + ¹³ C ¹⁶ O	¹² C ¹⁶ O + ¹² C ¹⁸ O	<i>R</i> (12/13)	<i>R</i> (16/18)	assignment
1992.9	1949.3	1944.9			1.0224	1.0247	(Y(CO) ₆)
1970.4	1927.9	1922.8			1.0220	1.0248	(Y(CO) ₅)
1946.4	1901.9	1899.8			1.0234	1.0245	(Y(CO) ₄)
1936.1	1894.5	1893.1			1.0220	1.0227	Y(CO) ₃
1919.6	1875.8	1873.6	1919.6, 1875.8	1919.6, 1873.6	1.0234	1.0246	YCO ⁺
1881.1	1840.3	1835.7	1881.0, 1866.8, 1851.4, 1840.3	1881.0, 1865.9, 1851.0, 1835.7	1.0222	1.0247	Y(CO) ₃
1858.9	1819.2	1815.5	1858.9, 1819.2	1858.9, 1815.5	1.0218	1.0239	YCO
1822.0	1782.8	1778.1	1822.0, 1797.1, 1782.8	1822.0, 1793.8, 1778.1	1.0220	1.0247	Y(CO) ₂ (bent)
1803.3	1764.2	1760.0	1803.3, 1783.4, 1764.2	1803.3, 1774.5, 1760.0	1.0222	1.0247	Y(CO) ₂ site
1791.2	1753.3	1748.8	1791.2, 1767.7, 1753.3	1791.2, 1764.7, 1748.8	1.0216	1.0242	Y(CO) ₂ (bent)

TABLE 3: Comparison of Observed and Calculated C–O Stretching Modes of the Lanthanum Carbonyls

species	$\nu_{\text{C-O}}$ mode	experimental			calculated			
		freq (cm ⁻¹)	<i>R</i> (12/13)	<i>R</i> (16/18)	method	freq (cm ⁻¹)	<i>R</i> (12/13)	<i>R</i> (16/18)
LaCO	σ	1814.0	1.0224	1.0245	BPW91	1841.7	1.0231	1.0243
(⁴ Σ^- , <i>C</i> _{∞v})					B3LYP	1901.3	1.0228	1.0246
LaCO ⁺	σ	1903.2	1.0221	1.0237	BPW91	1941.9	1.0229	1.0246
(³ Σ^- , <i>C</i> _{∞v})					B3LYP	2121.7	1.0228	1.0247
La(CO) ₂	a ₁	1776.0	1.0221	1.0249	BPW91	1877.6	1.0232	1.0242
(⁴ B ₂ , <i>C</i> _{2v})					B3LYP	1944.9	1.0229	1.0245
La(CO) ₂	b ₂	1745.6	1.0218	1.0253	BPW91	1833.9	1.0229	1.0245
(⁴ B ₂ , <i>C</i> _{2v})					B3LYP	1894.2	1.0227	1.0248
La(CO) ₂	σ	1788.2	1.0219	1.0251	BPW91	1893.9	1.0226	1.0252
(⁴ Σ_g^- , <i>D</i> _{∞h})					B3LYP	1964.5	1.0223	1.0254
La(CO) ₃	a ₁	1919.9	1.0218	1.0250	BPW91	1951.6	1.0258	1.0267
(⁴ A ₁ , <i>C</i> _{3v})					B3LYP	2029.7	1.0231	1.0243
La(CO) ₃	e	1849.9	1.0227	1.0241	BPW91	1877.3	1.0255	1.0274
(⁴ A ₁ , <i>C</i> _{3v})					B3LYP	1941.3	1.0225	1.0250
La(CO) ₄	e _u	1882.1	1.0220	1.0249	BPW91	1918.6	1.0225	1.0251
(⁴ B _{2g} , <i>D</i> _{4h})					B3LYP	1985.8	1.0223	1.0254

infrared spectra for the reactions of laser-ablated La and Y atoms with CO molecules in excess neon in the selected regions are illustrated in Figures 1–5, and the absorption bands in different isotopic experiments are listed in Tables 1 and 2. The stepwise annealing and photolysis behavior of the product absorptions is also shown in the figures and will be discussed below. Experiments were also done with different concentrations of CCl₄ serving as an electron scavenger in solid neon.

Quantum chemical calculations have been carried out for the possible isomers and electronic states of the potential product molecules. Interestingly, recent DFT calculations suggested the existence of isocarbonyls of Yb.²⁰ The present calculations indicated that the M(CO)_{*x*} and MCO⁺ (M = La, Y; *x* = 1–4) molecules are more stable than the isocarbonyls species, M(OC)_{*x*} and MOC⁺ (M = La, Y; *x* = 1–4). Furthermore, the calculated values of ν_{CO} in the M(CO)_{*x*} and MCO⁺ (M = La, Y; *x* = 1–4) molecules are much closer to the experimental values than those in the isocarbonyls species of La and Y. Herein, mainly the calculated results of the M(CO)_{*x*} and MCO⁺ (M = La, Y;

x = 1–4) molecules will be presented for discussion. Figure 6 shows the optimized structures of the reaction products. The comparison of the observed and calculated isotopic frequency ratios for the C–O stretching modes of lanthanum and yttrium carbonyls are summarized in Tables 3 and 4, respectively. The ground electronic states, point groups, vibrational frequencies (above 400 cm⁻¹), and intensities are listed in Table 5. Molecular orbital depictions of the highest occupied molecular orbitals (HOMOs) and HOMO-1 of the La(CO)_{*n*} (*n* = 1–4) and LaCO⁺ molecules are representatively illustrated in Figure 7.

MCO. In the La + CO experiments, the absorption at 1814.0 cm⁻¹ with a matrix trapping site at 1833.6 cm⁻¹ appears during sample deposition and markedly increases upon annealing qj (Table 1 and Figure 1). The main band (1814.0 cm⁻¹) shifts to 1774.2 cm⁻¹ with ¹³C¹⁶O and to 1770.6 cm⁻¹ with ¹²C¹⁸O, exhibiting isotopic frequency ratios (¹²C¹⁶O/¹³C¹⁶O, 1.0224; ¹²C¹⁶O/¹²C¹⁸O, 1.0245) characteristic of C–O stretching vibrations. As shown in Figure 2, the mixed ¹²C¹⁶O + ¹³C¹⁶O and

TABLE 4: Comparison of Observed and Calculated C–O Stretching Modes of the Yttrium Carbonyls

species	ν_{C-O} mode	experimental			calculated			
		freq (cm ⁻¹)	<i>R</i> (12/13)	<i>R</i> (16/18)	method	freq (cm ⁻¹)	<i>R</i> (12/13)	<i>R</i> (16/18)
YCO	σ	1858.9	1.0218	1.0239	BPW91	1822.2	1.0233	1.0239
(⁴ Σ^- , $C_{\infty v}$)					B3LYP	1874.1	1.0231	1.0242
YCO ⁺	σ	1919.6	1.0234	1.0246	BPW91	1933.4	1.0231	1.0242
(³ Σ^- , $C_{\infty v}$)					B3LYP	2013.8	1.0229	1.0247
Y(CO) ₂	a ₁	1822.0	1.0220	1.0247	BPW91	1871.3	1.0228	1.0247
(² B ₁ , C_{2v})					B3LYP	1961.2	1.0226	1.0250
Y(CO) ₂	b ₂	1791.2	1.0216	1.0242	BPW91	1837.3	1.0231	1.0243
(² B ₁ , C_{2v})					B3LYP	1910.3	1.0227	1.0248
Y(CO) ₃	a ₁	1936.1	1.0220	1.0227	BPW91	1948.6	1.0234	1.0237
(⁴ A ₁ , C_{3v})					B3LYP	2021.3	1.0233	1.0240
Y(CO) ₃	e	1881.1	1.0222	1.0247	BPW91	1871.1	1.0230	1.0243
(⁴ A ₁ , C_{3v})					B3LYP	1927.6	1.0228	1.0248
Y(CO) ₄	e _u	1946.4	1.0234	1.0245	BPW91	1909.5	1.0227	1.0250
(⁴ B _{2g} , D_{4h})					B3LYP	1957.3	1.0223	1.0255

TABLE 5: Ground Electronic States, Point Groups, Vibrational Frequencies (cm⁻¹) and Intensities (km/mol) of the Lanthanum and Yttrium Carbonyls Calculated at the BPW91/6-31+G(d)-CEP-31G Level (Only the Frequencies above 400 cm⁻¹ Are Listed)

species	elec state	point group	frequencies (intensity, mode)
LaCO	⁴ Σ^-	$C_{\infty v}$	1841.7 (1159, σ)
LaCO ⁺	³ Σ^-	$C_{\infty v}$	1941.9 (816, σ)
La(CO) ₂	⁴ B ₂	C_{2v}	1877.6 (844, A ₁), 1833.9 (1552, B ₂)
La(CO) ₂	⁴ Σ_g^-	$D_{\infty h}$	1960.4 (0, σ_g), 1893.9 (3490, σ_u)
La(CO) ₃	⁴ A ₁	C_{3v}	1951.6 (547, A ₁), 1877.3 (1599 × 2, E)
La(CO) ₄	⁴ B _{2g}	D_{4h}	2000.7 (0, A _{1g}), 1944.1 (0, B _{1g}), 1918.6 (3781 × 2, E _u)
YCO	⁴ Σ^-	$C_{\infty v}$	1822.2 (998, σ)
YCO ⁺	³ Σ^-	$C_{\infty v}$	1933.4 (676, σ)
Y(CO) ₂	² B ₁	C_{2v}	1871.3 (1924, A ₁), 1837.3 (693, B ₂), 424.0 (24, A ₁), 412.8 (8, B ₂)
Y(CO) ₂	⁴ Σ_g^-	$D_{\infty h}$	1956.7 (0, σ_g), 1876.0 (3450, σ_u)
Y(CO) ₃	⁴ A ₁	C_{3v}	1948.6 (487, A ₁), 1871.1 (1496 × 2, E)
Y(CO) ₄	⁴ B _{2g}	D_{4h}	2006.6 (0, A _{1g}), 1944.5 (0, B _{1g}), 1909.5 (3761 × 2, E _u)

¹²C¹⁶O + ¹²C¹⁸O isotopic spectra only provide the sum of pure isotopic bands, which indicates a monocarbonyl molecule.²¹ Doping with CCl₄ has no effect on this band (Figure 1, trace e), suggesting that the product is neutral.³ The 1814.0 and 1833.6 cm⁻¹ bands are therefore assigned to the C–O stretching vibration of the neutral lanthanum monocarbonyl LaCO in different matrix sites. The corresponding C–O stretching frequency of LaCO in solid argon has been observed at 1772.7 cm⁻¹,¹² which is 41.3 cm⁻¹ red-shifted from the present neon matrix counterpart (1814.0 cm⁻¹).

In the Y + CO experiments, the absorption of the analogous YCO molecule has been observed at 1858.9 cm⁻¹ (Table 2 and Figures 3–5). In the previous argon matrix experiments, two broad bands at 1874.1 and 1869.0 cm⁻¹ have been assigned to the YCO molecule.¹⁰

The previous calculations predicted that the CO molecule preferentially coordinates to the lanthanum atom with C end to form the linear metal carbonyl compound.^{12,22} Both BPW91 and B3LYP calculations predict that the LaCO and YCO molecules have a linear geometry (Figure 6) with a ⁴ Σ^- ground state. For the LaCO molecule, the C–O stretching frequency is calculated to be 1841.7 cm⁻¹ with the ¹²C¹⁶O/¹³C¹⁶O and ¹²C¹⁶O/¹²C¹⁸O isotopic frequency ratios of 1.0231 and 1.0243 at the BPW91/6-31+G(d)-CEP-31G level (Table 3), which are consistent with the experimental observations, respectively. The agreements between the experimental and calculated results have also been obtained at the B3LYP/6-31+G(d)-CEP-31G level (Table 3). Recent studies indicate that in most cases, the BPW91 functional gives calculated ν_{C-O} frequencies much closer to the experimental values than the B3LYP functional.^{3,4} Hereafter, mainly BPW91 results are presented for discussion.

M(CO)₂. The absorptions at 1776.0 and 1745.6 cm⁻¹ with La and CO in neon are present together upon sample annealing (Table 1 and Figure 1). These bands shift to 1737.6 and 1708.4 cm⁻¹ with ¹³C¹⁶O and to 1732.9 and 1702.6 cm⁻¹ with ¹²C¹⁸O, exhibiting isotopic frequency ratios (¹²C¹⁶O/¹³C¹⁶O, 1.0221 and 1.0218; ¹²C¹⁶O/¹²C¹⁸O, 1.0249 and 1.0253) characteristic of C–O stretching vibrations. As can be seen in Figure 2, two sets of triplet bands have been observed at 1774.3/1754.8/1737.9 and 1745.7/1723.4/1708.5 cm⁻¹ in the mixed ¹²C¹⁶O + ¹³C¹⁶O isotopic spectra (Table 1), suggesting that two equivalent CO subunits are involved in each mode.²¹ Similar isotopic spectra in the ¹²C¹⁶O + ¹²C¹⁸O experiments have also been obtained. Doping with CCl₄ has no effect on these bands (Figure 1, trace e), suggesting that the product is neutral.³ Accordingly, these bands are assigned to the symmetric and antisymmetric C–O stretching modes of the bent La(CO)₂ molecule.

The analogous features with Y and CO in neon weakly appear together during sample deposition at 1822.3 and 1791.2 cm⁻¹ and sharply increase upon annealing (Table 2, Figures 3 and 4). These two bands are assigned to the symmetric and antisymmetric C–O stretching modes of the bent Y(CO)₂ molecule on the basis of isotopic shifts and splitting patterns.

In the La + CO experiments, a weak band at 1788.2 cm⁻¹ appears during sample deposition and sharply increases after annealing (Table 1 and Figure 1). This band shifts to 1749.9 cm⁻¹ with ¹³C¹⁶O and to 1744.5 cm⁻¹ with ¹²C¹⁸O, exhibiting isotopic frequency ratios (¹²C¹⁶O/¹³C¹⁶O, 1.0219; ¹²C¹⁶O/¹²C¹⁸O, 1.0251) characteristic of C–O stretching vibrations. The 1:2:1 triplet patterns observed in both mixed ¹²C¹⁶O + ¹³C¹⁶O and ¹²C¹⁶O + ¹²C¹⁸O isotopic spectra imply that two equivalent CO

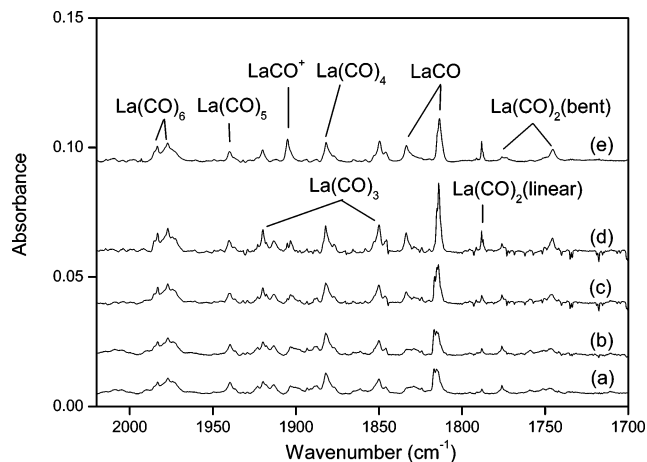


Figure 1. Infrared spectra in the 2000–1700 cm^{-1} region from co-deposition of laser-ablated La atoms with 0.3% CO in Ne. (a) After 1 h sample deposition at 4 K, (b) after annealing to 8 K, (c) after annealing to 10 K, (d) after annealing to 11 K, and (e) 0.3% CO + 0.05% CCl_4 , after annealing to 11 K.

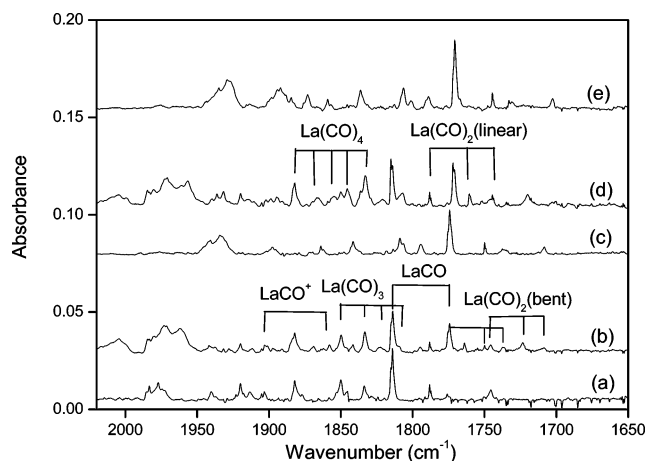


Figure 2. Infrared spectra in the 2000–1650 cm^{-1} region from co-deposition of laser-ablated La atoms with isotopic CO in Ne after annealing to 11 K. (a) 0.3% $^{12}\text{C}^{16}\text{O}$, (b) 0.2% $^{12}\text{C}^{16}\text{O}$ + 0.2% $^{13}\text{C}^{16}\text{O}$, (c) 0.3% $^{13}\text{C}^{16}\text{O}$, (d) 0.2% $^{12}\text{C}^{16}\text{O}$ + 0.2% $^{12}\text{C}^{18}\text{O}$, and (e) 0.3% $^{12}\text{C}^{18}\text{O}$.

subunits are involved in this mode.²¹ Doping with CCl_4 has no effect on this band (Figure 1, trace e), suggesting that the product is neutral.³ By analogy with linear $\text{Sc}(\text{CO})_2$ and $\text{Fe}(\text{CO})_2$ spectra,^{10,23} the 1788.2 cm^{-1} band is assigned to the antisymmetric C–O stretching mode of linear $\text{La}(\text{CO})_2$. The yttrium counterpart is absent from the present neon experiments.

DFT calculations have been performed for the $\text{La}(\text{CO})_2$ and $\text{Y}(\text{CO})_2$ molecules to support the above assignments. Both doublet and quartet states of the bent and linear $\text{La}(\text{CO})_2$ and $\text{Y}(\text{CO})_2$ molecules are found to be very close in energy. For the $\text{La}(\text{CO})_2$ molecule, the $^4\text{B}_2$ state lies 3, 9, and 4 kcal/mol in energy lower than the $^2\text{B}_1$, $^2\Pi_g$, and $^4\Sigma_g^-$ ones, respectively. For the $\text{Y}(\text{CO})_2$ molecule, the $^2\text{B}_1$ state lies 5, 10, and 2 kcal/mol in energy lower than the $^4\text{B}_2$, $^2\Pi_g$, and $^4\Sigma_g^-$ ones, respectively. The symmetric and antisymmetric C–O stretching vibrational frequencies of the $^4\text{B}_2$ $\text{La}(\text{CO})_2$ molecule are calculated at 1877.6 and 1833.9 cm^{-1} (Table 3), respectively, which should be scaled down by 0.946 and 0.952 to fit the experimental frequencies, 1776.0 and 1745.6 cm^{-1} . Such large discrepancy for the C–O stretching vibrational frequencies of the lanthanide carbonyls may be due to the inefficiency of the XC functional and/or the basis sets used here. For the antisymmetric C–O stretching mode, the calculated $^{12}\text{C}^{16}\text{O}/^{13}\text{C}^{16}\text{O}$ and $^{12}\text{C}^{16}\text{O}/^{12}\text{C}^{18}\text{O}$ isotopic frequency ratios of 1.0229 and 1.0245

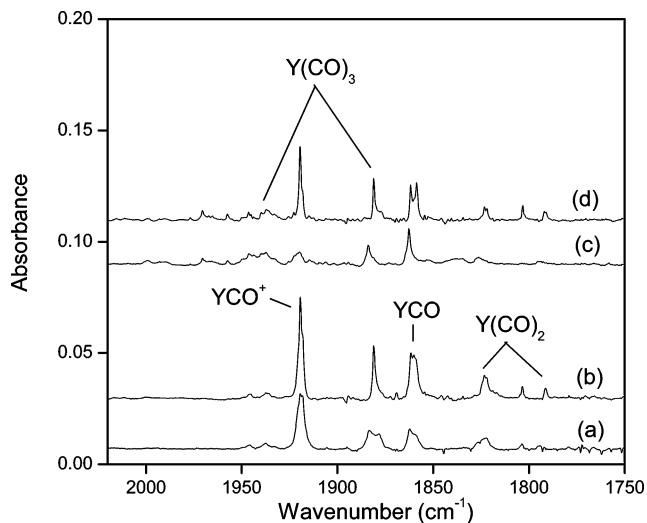


Figure 3. Infrared spectra in the 2000–1750 cm^{-1} region from co-deposition of laser-ablated Y atoms with 0.1% CO in Ne. (a) After 30 min of sample deposition at 4 K, (b) after annealing to 10 K, (c) after 10 min of broadband irradiation, and (d) after annealing to 11 K.

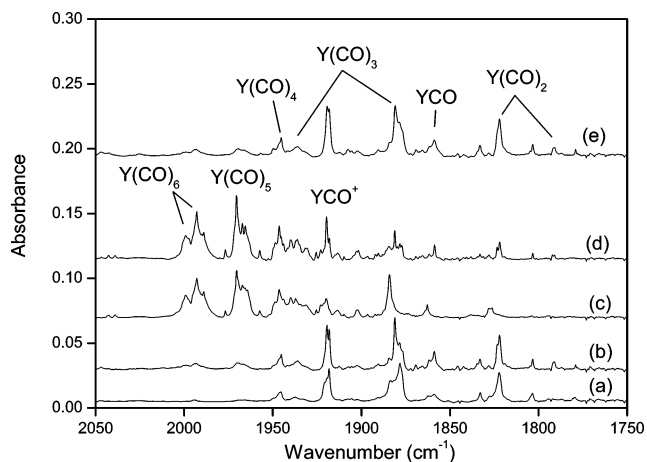


Figure 4. Infrared spectra in the 2050–1750 cm^{-1} region from co-deposition of laser-ablated Y atoms with 0.3% CO in Ne. (a) After 30 min sample deposition at 4 K, (b) after annealing to 10 K, (c) after 10 min of broadband irradiation, (d) after annealing to 11 K, and (e) 0.3% CO + 0.03% CCl_4 , after annealing to 10 K.

(Table 3) are consistent with the experimental observations, 1.0218 and 1.0253, respectively. Similar results have also been obtained for the $\text{Y}(\text{CO})_2$ molecule (Table 4 and Figure 6).

$\text{M}(\text{CO})_3$. In the reactions of laser-ablated La atoms with CO, the 1919.9 and 1849.9 cm^{-1} bands weakly appear together during sample deposition and visibly increase on sample annealing (Table 1 and Figure 1). The absorption at 1849.9 cm^{-1} shifts to 1808.9 cm^{-1} with $^{13}\text{C}^{16}\text{O}$ and to 1806.4 cm^{-1} with $^{12}\text{C}^{18}\text{O}$, exhibiting isotopic frequency ratios ($^{12}\text{C}^{16}\text{O}/^{13}\text{C}^{16}\text{O}$, 1.0227; $^{12}\text{C}^{16}\text{O}/^{12}\text{C}^{18}\text{O}$, 1.0241) characteristic of C–O stretching vibrations. The mixed isotopic spectra (Table 1 and Figure 2) are quartets with approximately 3:1:1:3 relative intensities, which are characteristic of doubly degenerate vibrational mode for a trigonal species.²¹ The intermediate component of the 1919.9 cm^{-1} band could be overlapped by other absorptions in the mixed isotopic spectra (Figure 2). Doping with CCl_4 has no effect on these bands (Figure 1, trace e), suggesting that the product is neutral.³ The 1919.9 and 1849.9 cm^{-1} bands are assigned to the symmetric and antisymmetric C–O stretching vibrations of the $\text{La}(\text{CO})_3$ molecule. The corresponding C–O stretching frequencies of the analogous $\text{Y}(\text{CO})_3$ product have

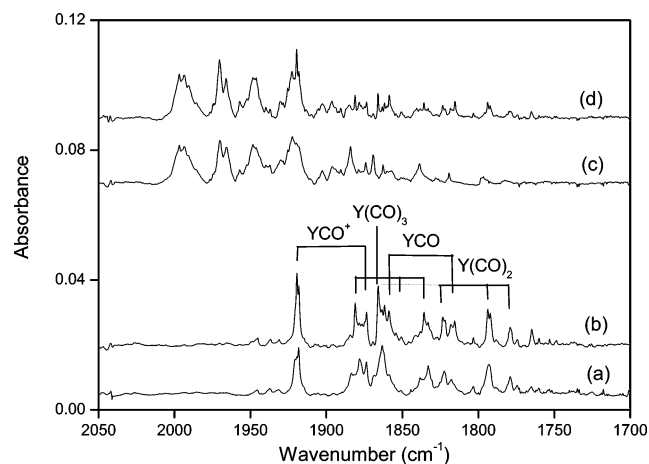


Figure 5. Infrared spectra in the 2050–1700 cm^{-1} region from co-deposition of laser-ablated Y atoms with 0.15% $^{16}\text{C}^{16}\text{O}$ + 0.15% $^{18}\text{C}^{18}\text{O}$ in Ne. (a) After 30 min of sample deposition at 4 K, (b) after annealing to 10 K, (c) after 10 min of broad-band irradiation, and (d) after annealing to 11 K.

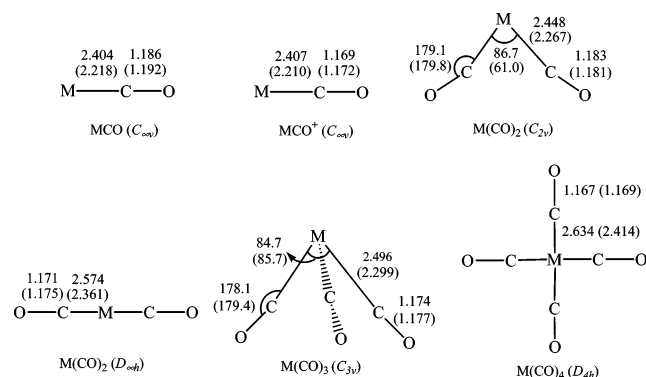


Figure 6. Optimized structures (bond lengths in angstroms, bond angles in degrees) of the lanthanum and yttrium (in parentheses) carbonyls calculated at the BPW91/6-31+G(d)-CEP-31G level.

been observed at 1936.1 and 1881.1 cm^{-1} in solid neon (Table 2, Figures 3 and 4). The previous argon matrix experiments give the absorptions of the scandium counterpart at 1968.0 and 1822.2 cm^{-1} .¹⁰

The assignment is supported by the present DFT calculations. The $\text{La}(\text{CO})_3$ and $\text{Y}(\text{CO})_3$ molecules are predicted to have C_{3v} symmetry with an 4A_1 ground electronic state (Tables 3–5 and Figure 6), similar to the $\text{Sc}(\text{CO})_3$ molecule.¹⁰ Taking the calculated results of the $\text{La}(\text{CO})_3$ molecule as an example, the symmetric and antisymmetric C–O stretching vibrational frequencies are calculated at 1951.6 and 1877.3 cm^{-1} (Tables 3 and 5), which agree with the experimental frequencies, 1919.6 and 1848.9 cm^{-1} , respectively. For the antisymmetric C–O stretching mode, the calculated $^{12}\text{C}^{16}\text{O}/^{13}\text{C}^{16}\text{O}$ and $^{12}\text{C}^{16}\text{O}/^{12}\text{C}^{18}\text{O}$ isotopic frequency ratios of 1.0255 and 1.0274 (Table 3) are consistent with the experimental observations, 1.0227 and 1.0241, respectively. Similar results have also been obtained for the $\text{Y}(\text{CO})_3$ molecule (Tables 4 and 5 and Figure 6).

$\text{M}(\text{CO})_4$. The 1882.1 cm^{-1} band with La and CO in neon appears during sample deposition and visibly increases on sample annealing (Table 1 and Figure 1). This band shifts to 1841.5 cm^{-1} with $^{13}\text{C}^{16}\text{O}$ and to 1836.3 cm^{-1} with $^{12}\text{C}^{18}\text{O}$, exhibiting isotopic frequency ratios ($^{12}\text{C}^{16}\text{O}/^{13}\text{C}^{16}\text{O}$, 1.0220; $^{12}\text{C}^{16}\text{O}/^{12}\text{C}^{18}\text{O}$, 1.0249) characteristic of C–O stretching vibrations. As can be seen in Figure 2, quintet isotopic patterns have

been observed at 1882.1/1869.1/1858.0/1849.9/1841.6 and 1882.1/1866.7/1854.8/1845.6/1836.3 cm^{-1} in the mixed $^{12}\text{C}^{16}\text{O}$ + $^{13}\text{C}^{16}\text{O}$ and $^{12}\text{C}^{16}\text{O}$ + $^{12}\text{C}^{18}\text{O}$ experiments (Table 1), respectively, which are the characteristic feature for the triply degenerate mode of a tetrahedral species.²¹ Doping with CCl_4 has no effect on this band (Figure 1, trace e), indicating that the product is neutral.³ Accordingly, the 1882.1 cm^{-1} band is assigned to the antisymmetric C–O stretching mode of the $\text{La}(\text{CO})_4$ molecule. Similar neon matrix experiments of Y and CO give the absorption of the analogous $\text{Y}(\text{CO})_4$ molecule at 1946.4 cm^{-1} (Table 2, Figure 4). The absorption of the $\text{Sc}(\text{CO})_4$ molecule has been observed at 1865.4 cm^{-1} in the previous argon matrix experiments.¹⁰

Our DFT calculations predict the $\text{La}(\text{CO})_4$ and $\text{Y}(\text{CO})_4$ molecules to have D_{4h} symmetry with a $^4B_{2g}$ ground electronic state (Tables 3–5 and Figure 6). For the $\text{La}(\text{CO})_4$ molecule, the antisymmetric C–O stretching vibrational frequency is calculated at 1918.6 cm^{-1} (Tables 3 and 5), which is consistent with the experimental value (1882.1 cm^{-1}). As summarized in Table 3, the calculated $^{12}\text{C}^{16}\text{O}/^{13}\text{C}^{16}\text{O}$ and $^{12}\text{C}^{16}\text{O}/^{12}\text{C}^{18}\text{O}$ isotopic frequency ratios of 1.0225 and 1.0251 (Table 3) are also in accord with the experimental observations, 1.0220 and 1.0249, respectively. Similar results have been obtained for the $\text{Y}(\text{CO})_4$ molecule (Tables 4 and 5 and Figure 6). These agreements between the experimental and calculated vibrational frequencies, relative absorption intensities, and isotopic shifts confirm the identifications of the $\text{La}(\text{CO})_4$ and $\text{Y}(\text{CO})_4$ molecules from the matrix IR spectra.

MCO^+ . In the La + CO experiments, the absorption at 1903.2 cm^{-1} appears during sample deposition and little changes after annealing (Table 1 and Figure 1). This band shifts to 1862.0 cm^{-1} with $^{13}\text{C}^{16}\text{O}$ and to 1859.1 cm^{-1} with $^{12}\text{C}^{18}\text{O}$, exhibiting isotopic frequency ratios ($^{12}\text{C}^{16}\text{O}/^{13}\text{C}^{16}\text{O}$, 1.0221; $^{12}\text{C}^{16}\text{O}/^{12}\text{C}^{18}\text{O}$, 1.0237) characteristic of C–O stretching vibrations. The mixed $^{12}\text{C}^{16}\text{O}$ + $^{13}\text{C}^{16}\text{O}$ and $^{12}\text{C}^{16}\text{O}$ + $^{12}\text{C}^{18}\text{O}$ isotopic spectra only provide the sum of pure isotopic bands (Figure 2), which indicates a monocarbonyl molecule.²¹ Doping with CCl_4 sharply increases this band (Figure 1, trace e), suggesting that the product is cationic.³ The 1903.2 cm^{-1} band is therefore assigned to the C–O stretching vibration of the LaCO^+ cation. The corresponding C–O stretching vibration of the YCO^+ cation in solid neon has been observed at 1919.6 cm^{-1} (Table 2 and Figures 3 and 4), which is 10.2 cm^{-1} blue-shifted from the argon matrix counterpart (1909.4 cm^{-1}).¹⁰ Similar neon and argon matrix experiments with scandium give the absorption of the ScCO^+ cation at 1962.4 and 1923.5 cm^{-1} , respectively.¹⁰

Our DFT calculations predict the LaCO^+ and YCO^+ molecules to have a $^3\Sigma^-$ ground state with $C_{\infty v}$ symmetry (Tables 3–5 and Figure 6). For the LaCO^+ molecule, the calculated C–O stretching mode is 1941.9 cm^{-1} (Table 3), which should be multiplied by 0.980 to fit the observed frequency. The calculated $^{12}\text{C}^{16}\text{O}/^{13}\text{C}^{16}\text{O}$ and $^{12}\text{C}^{16}\text{O}/^{12}\text{C}^{18}\text{O}$ isotopic frequency ratios of 1.0229 and 1.0246 are consistent with the experimental observations, 1.0221 and 1.0237, respectively (Table 3). Similar agreements have been obtained for the YCO^+ molecule (Tables 4 and 5 and Figure 6).

$\text{M}(\text{CO})_{5,6}$. The 1940.3, 1977.1, and 1983.3 cm^{-1} bands with La and CO in neon appear during sample deposition and visibly increase on sample annealing and show carbonyl C–O stretching vibrational frequency ratios (Table 1 and Figure 1). In the mixed isotopic experiments (Figure 2), complicated bands were observed, which are too difficult to be resolved and are tentatively assigned to the $\text{La}(\text{CO})_5$ and $\text{La}(\text{CO})_6$ molecules, respectively. Analogous potential $\text{Y}(\text{CO})_5$ and $\text{Y}(\text{CO})_6$ molecules

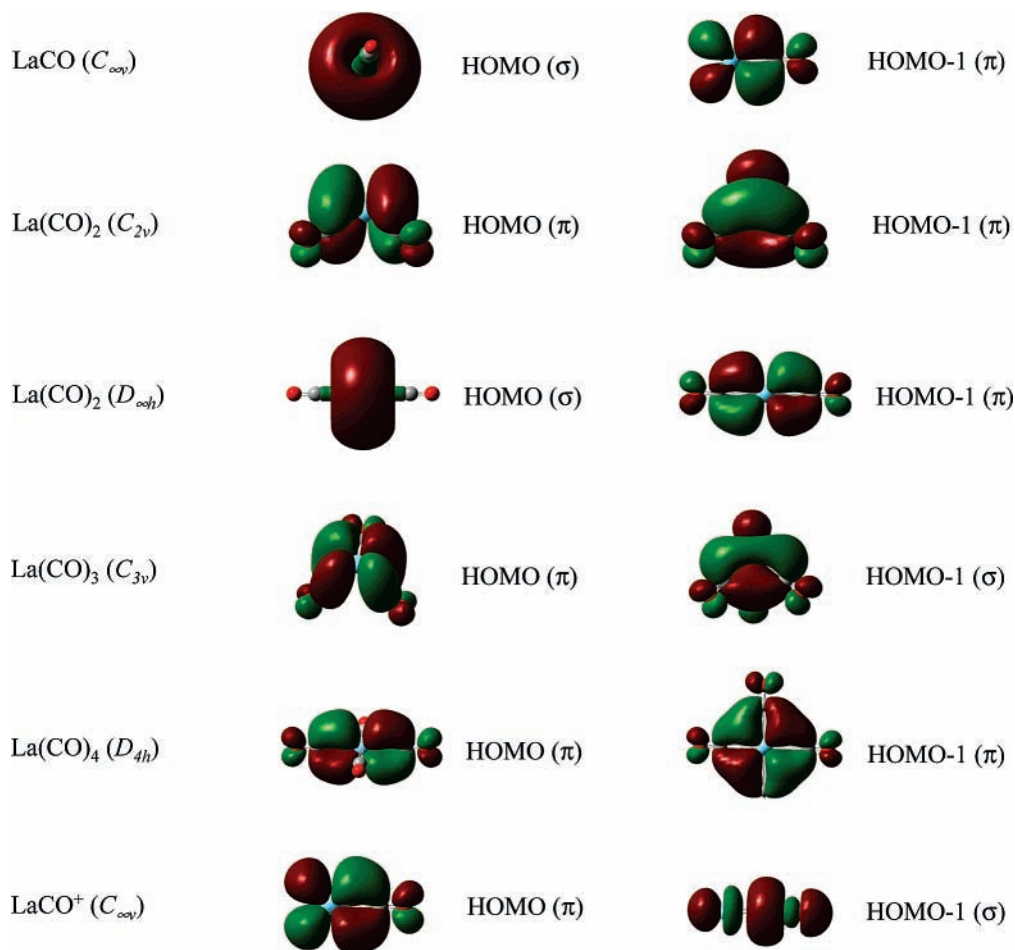
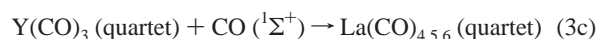
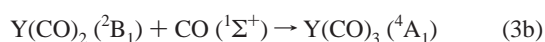
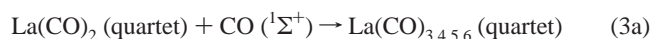
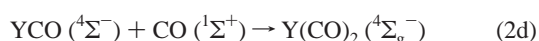
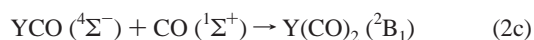
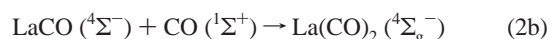
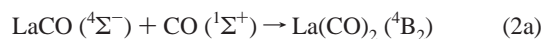


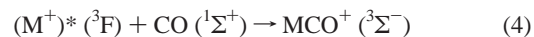
Figure 7. Molecular orbital depictions of the highest occupied molecular orbitals (HOMOs) and HOMO-1s of the $\text{La}(\text{CO})_n$ ($n = 1-4$) and LaCO^+ molecules

have been observed at 1970.4 and 1992.9 cm^{-1} in the present experiments (Table 2 and Figure 4).

Reaction Mechanism. At the present experimental conditions, laser-ablated lanthanum and yttrium atoms react with carbon monoxide molecules in the neon matrices to produce metal carbonyl species. The LaCO and YCO molecules appear during sample deposition and markedly increases upon annealing (Table 1 and Figure 1), suggesting that these products may be formed during the co-deposition of CO with laser-ablated metastable La and Y atoms (reaction 1a) or from the reactions of CO with ground state metal atoms upon annealing (reaction 1b). Higher metal carbonyls $\text{M}(\text{CO})_x$ ($\text{M} = \text{La}, \text{Y}; x = 2-6$) may be formed via the CO addition (reactions 2 and 3):



Recent investigations have shown that laser ablation of metal targets produces not only neutral metal atoms, but also metal cations and electrons, and ionic metal complexes can also be formed in the reactions with small molecules.^{3,4} In the present experiments, the MCO^+ ($\text{M} = \text{La}, \text{Y}$) cations appear during sample deposition and little change after sample annealing (Figures 1 and 4), suggesting that these cations may be generated during the co-deposition of laser-ablated M^+ cations with CO (reaction 4):



It is interesting to compare the observed C–O stretching vibrational frequencies of MCO^+ ($\text{M} = \text{Sc}, \text{Y}, \text{and La}$) in solid neon. The C–O stretching vibrational frequencies of MCO^+ decrease from Sc to La (1962.4, 1916.6, and 1903.2 cm^{-1}), which indicates an increasing in metal d orbital \rightarrow CO π^* back-donation in this series. Similar decrease trend in metal carbonyl frequencies going down the group 3 metals is also found for the early transition metals (groups 4–6),^{24–26} but the reverse trend for the late transition metals (groups 8–10).^{23,25,27–29} As early reported, DFT calculations could reproduce these trends well.

As illustrated in Figure 7, the HOMOs in the linear LaCO and $\text{La}(\text{CO})_2$ molecules are largely La 6s in character and the HOMO-1s are degenerate of π -type and mainly result from the contributions between the La 5d and C 2p atomic orbitals. The HOMOs in the $\text{La}(\text{CO})_2$ (bent), $\text{La}(\text{CO})_{3,4}$, and LaCO^+ molecules are the M–C π bonding orbitals. As can be seen from

the HOMO-1 in the bent La(CO)₂ molecule with the acute \angle CLaC, the carbon atoms of the CO ligands are close enough proximity to produce a significant C–C bonding interaction, which facilitates the back-donation from La atom to the CO ligands. Similar features can be found in the La(CO)₃ and La(CO)₄ molecules. Analogously, it has been reported that the Th(CO)_n ($n = 2-4$) molecules also adopt low-symmetry structures.³⁰

Conclusions

Reactions of laser-ablated lanthanum and yttrium atoms with carbon monoxide molecules in solid neon have been investigated using matrix-isolation infrared spectroscopy. In the lanthanum experiments, the absorptions at 1814.0, 1776.0, 1745.6, 1919.9, 1849.9, 1882.1, and 1903.2 cm⁻¹ are assigned to the C–O stretching vibrations of the LaCO, La(CO)₂, La(CO)₃, La(CO)₄, and LaCO⁺ molecules, respectively, on the basis of isotopic shifts, mixed isotopic splitting patterns, and CCl₄-doping experiments. Analogous Y(CO)_x and YCO⁺ ($x = 1-4$) products have been observed in the yttrium experiments. Density functional theory calculations have been performed on these lanthanum and yttrium carbonyls, which support the identifications of these carbonyls from the matrix infrared spectra. The present study reveals that the C–O stretching vibrational frequencies of MCO⁺ decrease from Sc to La, which indicates an increasing in metal d orbital \rightarrow CO π^* back-donation in this series.

Acknowledgment. We gratefully acknowledge financial support for this research by a Grant-in-Aid for Scientific Research (B) (Grant No. 17350012) from the Ministry of Education, Culture, Sports, Science and Technology (MEXT) of Japan. L.J. thanks MEXT of Japan and Kobe University for Honors Scholarship.

References and Notes

- (1) Cotton, F. A.; Wilkinson, G.; Murillo, C. A.; Bochmann, M. *Advanced Inorganic Chemistry*, 6th ed.; Wiley: New York, 1999.
- (2) Muettterties, E. L.; Stein, J. *Chem. Rev.* **1979**, *79*, 479.
- (3) Zhou, M. F.; Andrews, L.; Bauschlicher, C. W. Jr. *Chem. Rev.* **2001**, *101*, 1931, and references therein.
- (4) Himmel, H. J.; Downs, A. J.; Greene, T. M. *Chem. Rev.* **2002**, *102*, 4191, and references therein.
- (5) Xu, Q. *Coord. Chem. Rev.* **2002**, *231*, 83, and references therein.
- (6) Frenking, G.; Frohlich, N. *Chem. Rev.* **2000**, *100*, 717, and references therein.
- (7) Bridgeman, A. J. *Inorg. Chim. Acta* **2001**, *321*, 27.
- (8) See, for example: Xu, C.; Manceron, L.; Perchard, J. P. *J. Chem. Soc., Faraday Trans.* **1993**, *89*, 1291. Bondybey, V. E.; Smith, A. M.; Agreiter, J. *Chem. Rev.* **1996**, *96*, 2113. Fedrigo, S.; Haslett, T. L.; Moskovits, M. *J. Am. Chem. Soc.* **1996**, *118*, 5083. Khriachtchev, L.;

- Pettersson, M.; Runeberg, N.; Lundell, J.; Rasanen, M. *Nature* **2000**, *406*, 874. Himmel, H. J.; Manceron, L.; Downs, A. J.; Pullumbi, P. *J. Am. Chem. Soc.* **2002**, *124*, 4448. Li, J.; Bursten, B. E.; Liang, B.; Andrews, L. *Science* **2002**, *295*, 2242. Andrews, L.; Wang, X. *Science* **2003**, *299*, 2049.
- (9) Zhou, M. F.; Tsumori, N.; Li, Z.; Fan, K.; Andrews, L.; Xu, Q. *J. Am. Chem. Soc.* **2002**, *124*, 12936. Zhou, M. F.; Xu, Q.; Wang, Z.; von Ragué Schleyer, P. *J. Am. Chem. Soc.* **2002**, *124*, 14854. Xu, Q.; Jiang, L.; Tsumori, N. *Angew. Chem., Int. Ed.* **2005**, *44*, 4338. Jiang, L.; Xu, Q. *J. Am. Chem. Soc.* **2005**, *127*, 8906.
 - (10) Zhou, M. F.; Andrews, L. *J. Phys. Chem. A* **1999**, *103*, 2964.
 - (11) Jiang, L.; Xu, Q. *J. Am. Chem. Soc.* **2005**, *127*, 42.
 - (12) Xu, Q.; Jiang, L.; Zou, R.-Q. *Chem. Eur. J.* **2006**, *12*, 3226.
 - (13) Jiang, L.; Xu, Q. *J. Phys. Chem. A* **2006**, *110*, 5636.
 - (14) Burkholder, T. R.; Andrews, L. *J. Chem. Phys.* **1991**, *95*, 8697.
 - (15) Zhou, M. F.; Tsumori, N.; Andrews, L.; Xu, Q. *J. Phys. Chem. A* **2003**, *107*, 2458. Jiang, L.; Xu, Q. *J. Chem. Phys.* **2005**, *122*, 034505.
 - (16) Frisch, M. J.; Trucks, G. W.; Schlegel, H. B.; Scuseria, G. E.; Robb, M. A.; Cheeseman, J. R.; Montgomery, Jr., J. A.; Vreven, T.; Kudin, K. N.; Burant, J. C.; Millam, J. M.; Iyengar, S. S.; Tomasi, J.; Barone, V.; Mennucci, B.; Cossi, M.; Scalmani, G.; Rega, N.; Petersson, G. A.; Nakatsuji, H.; Hada, M.; Ehara, M.; Toyota, K.; Fukuda, R.; Hasegawa, J.; Ishida, M.; Nakajima, T.; Honda, Y.; Kitao, O.; Nakai, H.; Klene, M.; Li, X.; Knox, J. E.; Hratchian, H. P.; Cross, J. B.; Adamo, C.; Jaramillo, J.; Gomperts, R.; Stratmann, R. E.; Yazyev, O.; Austin, A. J.; Cammi, R.; Pomelli, C.; Ochterski, J. W.; Ayala, P. Y.; Morokuma, K.; Voth, G. A.; Salvador, P.; Dannenberg, J. J.; Zakrzewski, V. G.; Dapprich, S.; Daniels, A. D.; Strain, M. C.; Farkas, O.; Malick, D. K.; Rabuck, A. D.; Raghavachari, K.; Foresman, J. B.; Ortiz, J. V.; Cui, Q.; Baboul, A. G.; Clifford, S.; Cioslowski, J.; Stefanov, B. B.; Liu, G.; Liashenko, A.; Piskorz, P.; Komaromi, I.; Martin, R. L.; Fox, D. J.; Keith, T.; Al-Laham, M. A.; Peng, C. Y.; Nanayakkara, A.; Challacombe, M.; Gill, P. M. W.; Johnson, B.; Chen, W.; Wong, M. W.; Gonzalez, C.; Pople, J. A. *Gaussian 03*, revision B.04; Gaussian, Inc.: Pittsburgh, PA, 2003.
 - (17) Becke, A. D. *Phys. Rev. A* **1988**, *38*, 3098. Perdew, J. P.; Burke, K.; Wang, Y. *Phys. Rev. B* **1996**, *54*, 16533. Lee, C.; Yang, E.; Parr, R. G. *Phys. Rev. B* **1988**, *37*, 785. Becke, A. D. *J. Chem. Phys.* **1993**, *98*, 5648.
 - (18) McLean, A. D.; Chandler, G. S. *J. Chem. Phys.* **1980**, *72*, 5639. Krishnan, R.; Binkley, J. S.; Seeger, R.; Pople, J. A. *J. Chem. Phys.* **1980**, *72*, 650. Frisch, M. J.; Pople, J. A.; Binkley, J. S. *J. Chem. Phys.* **1984**, *80*, 3265.
 - (19) Stevens, W.; Basch, H.; Krauss, J. *J. Chem. Phys.* **1984**, *81*, 6026. Stevens, W. J.; Krauss, M.; Basch, H.; Jasien, P. G. *Can. J. Chem.* **1992**, *70*, 612. Cundari, T. R.; Stevens, W. J. *J. Chem. Phys.* **1993**, *98*, 5555.
 - (20) Maron, L.; Perrin, L.; Eisenstein, O.; Andersen, R. A. *J. Am. Chem. Soc.* **2002**, *124*, 5614.
 - (21) Darling, J. H.; Ogden, J. S. *J. Chem. Soc., Dalton Trans.* **1972**, 2496.
 - (22) G. Hong, X. Lin, L. Li, G. Xu, *J. Phys. Chem. A* **1997**, *101*, 9314.
 - (23) Zhou, M. F.; Chertihin, G. V.; Andrews, L. *J. Chem. Phys.* **1998**, *109*, 10893.
 - (24) Zhou, M. F.; Andrews, L. *J. Am. Chem. Soc.* **2000**, *122*, 1531.
 - (25) Zhou, M. F.; Andrews, L. *J. Phys. Chem. A* **1999**, *103*, 5259.
 - (26) Andrews, L.; Zhou, M. F.; Gutsev, G. L.; Wang, X. F. *J. Phys. Chem. A* **2003**, *107*, 561. Andrews, L.; Zhou, M. F.; Gutsev, G. L. *J. Phys. Chem. A* **2003**, *107*, 990.
 - (27) Zhou, M. F.; Andrews, L. *J. Phys. Chem. A* **1999**, *103*, 6956.
 - (28) Zhou, M. F.; Andrews, L. *J. Phys. Chem. A* **1999**, *103*, 7773.
 - (29) Liang, B. Y.; Zhou, M. F.; Andrews, L. *J. Phys. Chem. A* **2000**, *104*, 3905.
 - (30) Zhou, M. F.; Andrews, L.; Li, J.; Bursten, B. E. *J. Am. Chem. Soc.* **1999**, *121*, 12188. Li, J.; Bursten, B. E.; Zhou, M. F.; Andrews, L. *Inorg. Chem.* **2001**, *40*, 5448.